Journal of Applied Polymer Science

Component Ratio Effects of Hyperbranched Triazine Compound and Ammonium Polyphosphate in Flame-Retardant Polypropylene Composites

Menglan Xu, Yajun Chen, Lijun Qian, Jingyu Wang, Shuo Tang
Department of Materials Science & Engineering, Beijing Technology and Business University, Beijing 100048, People's Republic of China
Correspondence to: L. Qian (E-mail: augusqian@163.com)

ABSTRACT: A hyperbranched derivative of triazine group (EA) was synthesized by elimination reaction between ethylenediamine and cyanuric chloride. The different-mass-ratio EA and ammonium polyphosphate (APP) were mixed and blended with polypropylene (PP) in a constant amount (25%) to prepare a series of EA/APP/PP composites. The component ratio effect of EA/APP on the flame-retardant property of the EA/APP/PP composites was investigated using the limiting oxygen index (LOI), vertical burning (UL-94), and cone calorimetry tests. Results indicated that the EA/APP/PP (7.50/17.50/75.00) composite with the appropriate EA/APP mass ratio had the highest LOI, UL94 V-0 rating, lowest heat release rate, and highest residue yield. These results implied that the appropriate EA/APP mass ratio formed a better intumescent flame-retardant system and adequately exerted their synergistic effects. Furthermore, average effective combustion heat values revealed that EA/APP flame retardant possessed the gaseous-phase flame-retardant effect on PP. Residues of the EA/APP/PP composites were also investigated by scanning electron microscopy, Fourier-transform infrared, and X-ray photoelectron spectroscopy. Results demonstrated that the appropriate EA/APP mass ratio can fully interact and lock more chemical constituents containing carbon and nitrogen in the residue, thereby resulting in the formation of a dense, compact, and intumescent char layer. This char layer exerted a condensed-phase flame-retardant effect on EA/APP/PP composites. © 2014 Wiley Periodicals, Inc. J. Appl. Polym. Sci. **2014**, *131*, 41006.

KEYWORDS: blends; flame retardance; polyolefins

Received 15 February 2014; accepted 12 May 2014
DOI: 10.1002/app.41006

INTRODUCTION

In recent years, intumescent flame retardants (IFRs) have been widely used in polyolefins (e.g., polypropylene (PP) and polyethylene) because of their outstanding advantages, such as low smoke, nontoxicity, no corrosive gas, no dripping and halogen-free, etc.[1–4] In general, IFR is mainly composed of three basic constituents, namely, acid source, charring agent, and blowing agent.[5] A classical component of IFR is the ammonium polyphosphate (APP)/pentaerythritol/melamine system, which has been given more attention and deeply investigated by several flame-retardant study groups.[6–8] However, the flame-retardant efficiency and thermal stability of traditional IFR additives still need further enhancement compared with bromine-containing flame retardants.[9] Commonly, the charring agents in IFR are polyols (e.g., pentaerythritol, dipentaerythritol, mannitol, and sorbitol), but their thermal stabilities, charring, and flame-retardant efficiencies are inadequate when they are applied in flame-retardant polyolefins.[10]

In order to increase the flame-retardant efficiency of IFR, many methods have already been utilized, such as addition of synergist zeolite in IFR additives, adjustment of the relative ratio among three components of IFR,[10] and synthesis of some novel charring agents with high thermal stability. In order to obtain more effective IFRs, two novel kinds of charring agents have been synthesized, namely, polyol phosphate compounds[11–13] and triazine derivatives.[14,15] However, small molecules containing triazine ring used as charring agents in IFR have to be improved in thermal stability, flame retardant efficiency, and migration onto the surface of the matrix.[5] In recent years, the hyperbranched and linear macromolecules containing triazine ring structures have received more attention because of their high thermal stability, charring, and flame-retardant efficiencies derived from the structural character of triazine ring.[16–18]

In this current work, a charring additive-hyperbranched derivative of triazine (EA) was synthesized and characterized. Then the EA/APP IFR was applied in PP to investigate its flame-

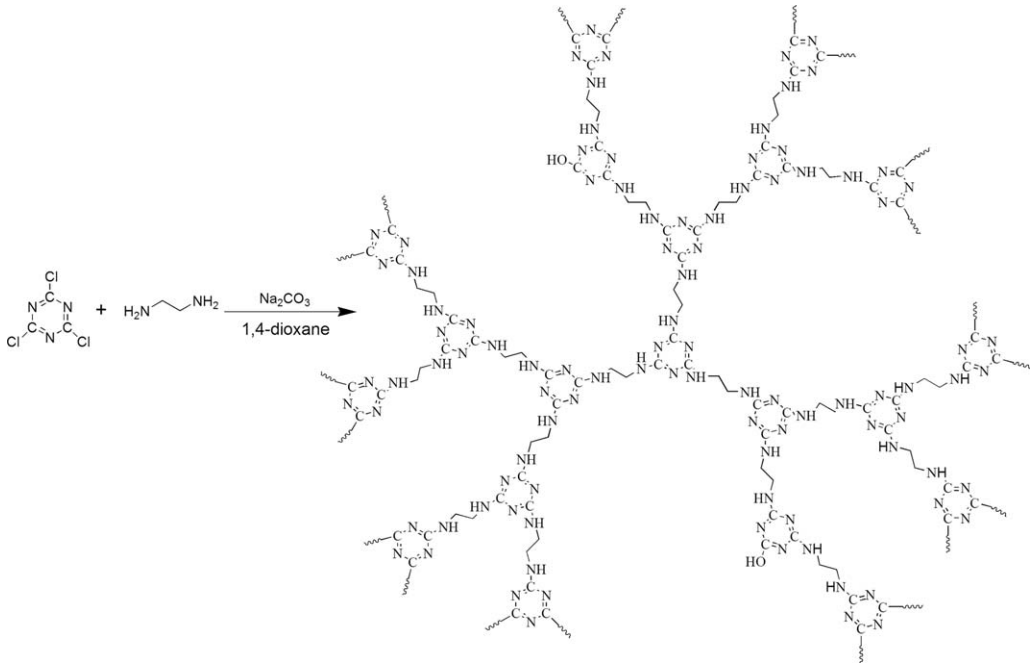

Scheme 1. Synthesis route of EA.

retardant properties. The flame-retardant component synergistic effects of EA and APP on PP were researched and the flame retardant synergistic mechanism was also studied.

EXPERIMENTAL

Materials

Ethylenediamine (analytical) was supplied by Tianjin Fuchen Chemical Reagents Factory, China. Cyanuric chloride (industrial) was purchased from Hebei Chengxin Chemical Co. Ltd., China. 1,4-Dioxane (analytical) and sodium carbonate anhydrous (Na_2CO_3, analytical) were purchased from Sinopharm Chemical Reagent Co. Ltd., China. PP (T30s; melt flow rate = 3.0 g/10 min) was provided by China National Petroleum Corporation, China. APP (average particle size = 15 μm; degree of polymerization > 1000) was purchased from Polyrocks Chemical Co., Ltd., China.

Instrumentation

Fourier-transform infrared (FTIR) spectra were obtained on a Nicolet iN10MX spectrometer using KBr pellets. ^{13}C solid-state NMR spectrum was recorded on a Bruker AVANCE III 400WB at 400 MHz.

The limiting oxygen index (LOI), with an error value of $\pm$0.5%, was obtained using an FTT (Fire Testing Technology, UK) Dynisco LOI instrument according to ASTM D2863-97 (sample size = 100.0 $\times$ 6.5 $\times$ 3.2 mm^3).

A UL-94 vertical burning test was performed on an FTT0082 instrument according to ANSL/UL-94–2009 (sample size = 130.0 $\times$ 13.0 $\times$ 3.2 mm^3).

A cone calorimetry test was performed using an FTT0007 cone calorimeter according to ISO5660 under an external heat flux of 50 kW/m^2 (sample size = 100.0 $\times$ 100.0 $\times$ 3.0 mm^3). The specimens were horizontally measured without any grid. Typical results from the cone calorimetry tests were reproducible to within $\pm$10%.

The surface morphologies of the residues after the cone calorimetry test with a conductive gold layer were observed using an FP 2032/14 Quanta 250 FEG scanning electron microscopy (SEM) system under a high vacuum at a voltage of 20 kV.

The elemental compositions of the residues were analyzed by X-ray photoelectron spectroscopy (XPS) on a PHI Quantera-II SXM (Ulvac-PHI, Inc.) using Al kα radiation and X-ray power of 2.5 kW under a vacuum of 2.6 $\times$ 10^{-7} Pa. The pass energy was 280 eV, and the step length was 1 eV with a takeoff angle of 45°. The relative error value was $\pm$5%.

Synthesis of Hyperbranched Derivative of Triazine (EA)

Exactly cyanuric chloride (55.35 g, 0.30 mol), Na_2CO_3 (104.94 g, 0.99 mol), and 450 mL 1,4-dioxane were fed into a 1000-mL three-necked flask equipped with a stirrer. The mixture was then stirred and cooled to 5°C in an ice-water bath. A solution of ethylenediamine (28.41 g, 0.47 mol) in 150 mL 1,4-dioxane was added dropwise to the mixture for 30 min with vigorous stirring while keeping the reaction mixture cool. The reacting mixture was stirred for another 3 h from 0°C to 20°C. After increasing the reaction temperature to 50°C and further to 100°C after 3 h, the reaction was carried out for another 3 h. The reaction mixture was filtered to remove the solvent, and the product was washed three times with hot water and dried in a vacuum oven at 100°C. A white powder product was obtained with a yield of 99.6%. The synthesis route is illustrated in Scheme 1.

Preparation of Flame-Retardant EA/APP/PP Composites

The IFR EA/APP was prepared by mixing APP and EA together at different mass ratios. Then, 25 wt % EA/APP and 75 wt % PP were blended in a torque rheometer at 180°C and 40 rpm

Table I. Formulas of EA/APP/PP Composites

Sample	Components (wt %)			EA (wt %)/APP (wt %)
	PP	EA	APP	
PP	100.00	0.00	0.00	
EA/APP/PP (1.25/23.75/75.00)	75.00	1.25	23.75	5/95
EA/APP/PP (2.50/22.50/75.00)	75.00	2.50	22.50	10/90
EA/APP/PP (3.75/21.25/75.00)	75.00	3.75	21.25	15/85
EA/APP/PP (5.00/20.00/75.00)	75.00	5.00	20.00	20/80
EA/APP/PP (6.25/18.75/75.00)	75.00	6.25	18.75	25/75
EA/APP/PP (7.50/17.50/75.00)	75.00	7.50	17.50	30/70
EA/APP/PP (8.75/16.25/75.00)	75.00	8.75	16.25	35/65

for 8 min. The formulae are presented in Table I. The EA/APP/PP composites were transferred to a mold, preheated at 170°C for 8 min, pressed at 170°C for the succeeding 6 min, and then cooled to room temperature while maintaining the pressure to obtain the composite sheets. The sheets were then cut into standard dimensions for further testing.

RESULTS AND DISCUSSION

Characterization of EA

The FTIR spectrum (KBr) exhibited absorptions at 3266 cm^{-1} (N—H), 2920 cm^{-1} and 2851 cm^{-1} (—CH_2—), 1612 cm^{-1} and 1558 cm^{-1} (triazine ring), and 1398 cm^{-1} (C—N). The characteristic groups, e.g. triazine ring, methylene, and amino, all appeared in the spectrum, which indicated that ethylenediamine were connected with cyanuric chloride and the compound, were obtained. The melting point cannot be detected by instruments because of the presence of hyperbranched macromolecule.

The structure of EA is also confirmed by ^{13}C solid-state NMR in Figure 1. The shift at 165.64 ppm and 40.39 ppm were attributed to C in the triazine ring and C in methylene, respectively. The other shifts weren't observed in the spectrum, which showed chlorine atoms in triazine ring were substituted by ethylenediamine group mostly. But a tiny amount of oxygen atoms were detected from the result of XPS and it disclosed that a few chlorine atoms weren't replaced and hydrolyzed to hydroxyl groups in the subsequent washing. Therefore, the compounds were identified as hyperbranched macromolecule.

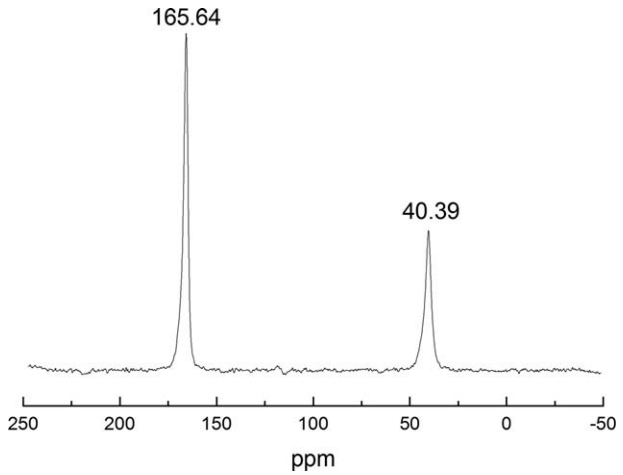

Figure 1. ^{13}C solid-state NMR spectrum of EA

LOI and UL94 Tests

LOI and UL-94 tests were carried out to evaluate the flame-retardant properties of EA/APP/PP composites. The results in Table II show that the flame-retardant ratings gradually increased to the UL94 V-0 level with increasing mass ratio of EA/APP. The IFR exhibited inferior flame-retardant properties, and the samples eventually burned to the clamp at a lower EA/APP mass ratio. However, with increased EA/APP mass ratio to the value between 3.75/21.25 and 8.75/16.25, the flame-retardant ratings reached to UL94 V-0. Similar to classical IFRs, the two components of the EA/APP system also exerted synergistic effects and brought the better flame-retardant properties when the EA/APP mass ratio was adjusted to a certain range. The LOI values disclosed the detailed changes with increased EA/APP mass ratio, as seen from the LOI data in Table II and the fitting curve in Figure 2. The LOI values initially increased and then decreased with increasing mass ratio of EA/APP, and when the mass ratio of EA/APP reached to 7.50/17.50, the LOI value reached the maximum value. The optimal EA/APP mass ratio was thus obtained. Therefore, the two components EA and APP exerted the best synergistic flame-retardant effect on PP at 7.50/17.50 EA/APP mass ratio. The action mechanism was subsequently analyzed.

Figure 3 shows the digital photos of EA/APP/PP residues after the burning test. During the test, all specimens were rotated and ignited with an alcohol lamp for 30 s. The amount and shape of residues formed during combustion were clearly observed. Figure 3(a,b) shows that a rare char was formed and had weak adhesive strength with the matrix, which resulted in poor flame retardancy and melt dripping. Figure 3(c–g) shows that a char layer was formed and that the thickness of this char layer increased with increasing mass ratio of EA/APP. Furthermore, adhesion between char layer and matrix was also strengthened, which contributed char to coating in the surface of matrix and further hindering the exchange of heat and flammable gas.[19] As a result, the flame-retardant properties of EA/APP/PP composites were enhanced.

Table II. LOI and UL-94 Results of Pure PP and EA/APP/PP Composites

	UL 94 vertical burning test				
Sample	t_1[a] (s)	t_2[b] (s)	Dripping	UL 94 rating	LOI (%)
PP	Burn[c]	/	Yes	No rating	17.5
EA/APP/PP (1.25/23.75/75.00)	16.2	Burn[c]	Yes	No rating	21.0
EA/APP/PP (2.50/22.50/75.00)	0	Burn[c]	Yes	No rating	25.8
EA/APP/PP (3.75/21.25/75.00)	0	2.8	No	V-0	29.3
EA/APP/PP (5.00/20.00/75.00)	0	4.1	No	V-0	31.6
EA/APP/PP (6.25/18.75/75.00)	0	3.4	No	V-0	32.0
EA/APP/PP (7.50/17.50/75.00)	0	0.0	No	V-0	32.3
EA/APP/PP (8.75/16.25/75.00)	0	0.0	No	V-0	30.2

[a] t_1 (s): maximum time of combustion in five specimens after the first ignition for 10 s.
[b] t_2 (s): maximum time of combustion in 5 specimens after the second ignition for 10 s.
[c] *Burn*: Burn to the clamp.

Cone Calorimetry Test

The heat release rate (HRR) curves and mass loss rate (MLR) curves measured by cone calorimetry are illustrated in Figures 4 and 5. Table III shows the first HRR peak value (PHRR1), the second HRR peak value (PHRR2), and the average value of HRR (av-HRR) of EA/APP/PP composites. With increased EA/APP mass ratio, the PHRR1 and Av-HRR of EA/APP/PP composites initially decreased and then increased, corresponding to the change trend of LOI results. This phenomenon indicated that the combustion intensity was being increasingly restrained and that the ternary synergistic interaction of EA/APP IFR was gradually optimized as the EA/APP mass ratio reached 7.50/17.50. However, a further increase in EA/APP mass ratio led to a reduction in PHRR1 value, indicating that the optimal balance of ternary synergistic interaction was destroyed. The HRR curves (Figure 4) showed that neat PP exhibited only one peak in HRR curves, whereas the EA/APP/PP composites possessed two HRR peaks that were dramatically reduced when EA/APP flame retardant was incorporated into the composites. Direct observations revealed that the two HRR peaks resulted from the formation and breaking of the char layer. Moreover, the PHRR1 was attributed to the initial formation of the intumescent char layer. In addition, when tested under heat flux, the surface of EA/APP/PP composites gradually produced the char layer and inhibited the heat from pyrolyzing the underlying matrix. This phenomenon weakened the thermal degradation of the matrix and reduced the HRR peak value. However, further heating caused fine cracks to gradually emerge on the char layer surface and resulted in the release of flammable gas from matrix interior. Consequently, combustion intensity was simultaneously enhanced and PHRR2 appeared.[20] PHRR2 did not only decrease but was also delayed with increasing mass ratio of EA/APP, indicating that more compact and stable char layers were gradually generated on the surface of EA/APP/PP composites because of the optimized EA/APP mass ratio.

Taking into consideration the pyrolysis behavior of the EA/APP/PP composites, the normalized MLR curves from cone calorimeter are illustrated in Figure 5. MLR represents the gasifying decomposition rate of the matrix. Figure 5(a,b) shows that all MLRs of the composites were gradually reduced and correspondingly the residue yields at 650 s increased with increasing EA/APP mass ratio from 1.25/23.75 to 7.50/17.50. With further

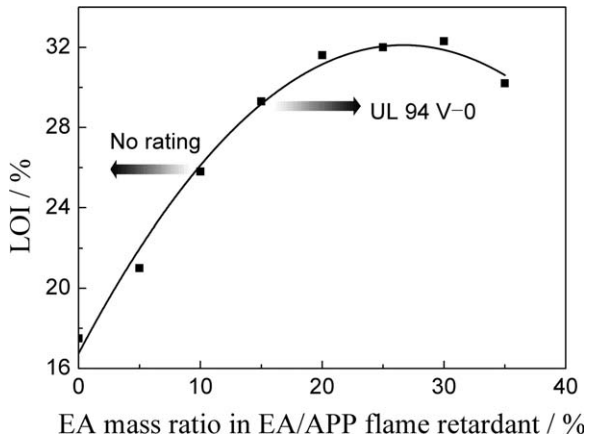

Figure 2. Fitting curve of LOI value.

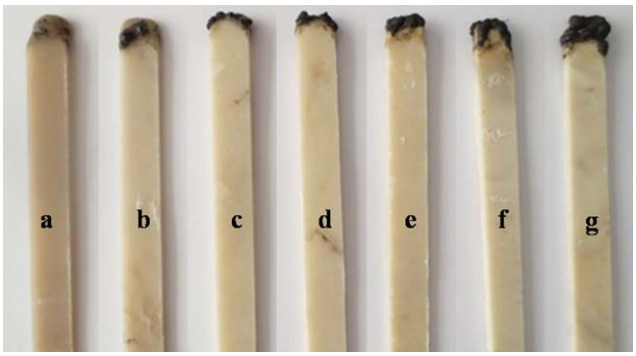

Figure 3. Digital photos of EA/APP/PP composites after horizontal flame test (a) EA/APP/PP (1.25/23.75/75.00), (b) EA/APP/PP(2.50/22.50/75.00), (c) EA/APP/PP(3.75/21.25/75.00), (d) EA/APP/PP(5.00/20.00/75.00), (e) EA/APP/PP(6.25/18.75/75.00), (f) EA/APP/PP(7.50/17.50/75.00), and (g) EA/APP/PP(8.75/16.25/75.00). [Color figure can be viewed in the online issue, which is available at wileyonlinelibrary.com.]

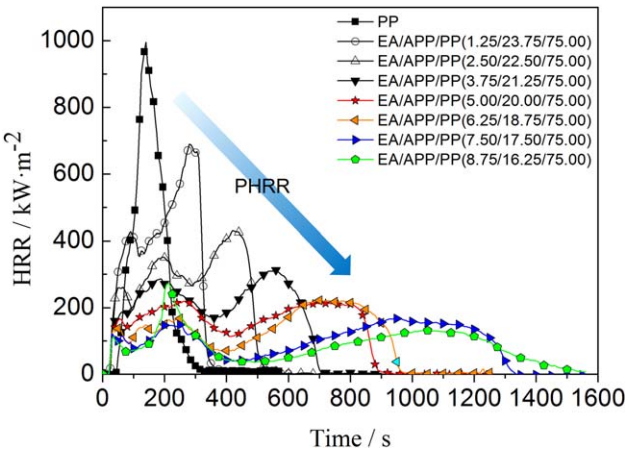

Figure 4. HRR curves of pure PP and EA/APP/PP composites. [Color figure can be viewed in the online issue, which is available at wileyonlinelibrary.com.]

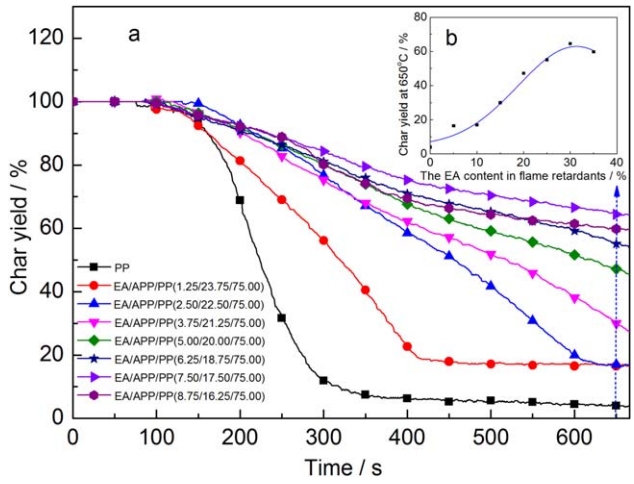

Figure 5. (a) Normalized MLR curves of EA/APP/PP composites from the cone calorimetry test. (b) Fitting curve of residue char yields of EA/APP/PP composites at 650 s from the cone calorimetry test. [Color figure can be viewed in the online issue, which is available at wileyonlinelibrary.com.]

increased EA/APP mass ratio to 8.75/16.25, the MLR and residue yields all turned to the opposite trends. These results suggested that the increased EA/APP mass ratio in the composites from 1.25/23.75 to 7.50/17.50 promoted charring, which preserved more constituents in the residue and enhanced the residue weight. However, the higher 8.75/16.25 EA/APP mass ratio was detrimental to charring. Regarding IFRs, higher residue yields effectively hindered heat from decomposing the underlying matrix, which resulted in better flame retardancy. The EA/APP mass ratio with the lowest MLR and the highest residue char yields correspond to the mass ratio with the best flame retardancy. Therefore, the 7.50/17.50 EA/APP mass ratio contributed to fully exerting the synergistic charring effect of EA and APP, accordingly enhancing the flame-retardant performance.

Av-EHC (effective combustion heat), which is the ratio of av-HRR to the average MLR (av-MLR) from the cone calorimetry test, discloses the burning rate of volatile gases in gaseous-phase flame during combustion and benefits the analysis of the action mechanism of flame retardants. From the EA/APP mass ratios of 1.25/23.75 to 8.75/16.25, the av-EHC initial values gradually decreased to the minimum value of EA/APP/PP (7.50/17.50/75.00) composites and then slightly increased. This trend of av-EHC values was the same as those of av-PHRR and av-MLR, but the reduction of av-EHC meant that av-PHRR more rapidly decreased than av-MLR, indicating that EA/APP flame retardant with the appropriate mass ratio played a more remarkably gaseous-phase flame-retardant role. In the gaseous phase, some APP molecules decomposed into phosphorous free radicals (i.e., volatiles) to capture oxygen and alkane free radicals, thereby inhibiting the burning process. When the mass ratio of EA/APP exceeded 7.50/17.50, the av-PHRR and av-MLR values all turned to increase, but the av-PHRR more significantly increased than av-MLR. Accordingly, the av-EHC slightly enhanced. Therefore, two deductions can be made. First, the IFR EA/APP possessed both condensed- and gaseous-phase flame-retardant effects; second, the IFR EA/APP with 7.50/17.50 mass ratio had the best flame-retardant performance because of the optimal combination of condensed- and gaseous-phase flame-retardant effects.

Table III reveals that the addition of EA/APP flame retardant shortened the time to ignition (TTI) values of all the composites. It can be ascribed to the degradation of EA/APP in advance while heating, which induced matrix decomposition and released the flammable gas, causing the TTI shortening. However, the advanced decomposition of the flame retardant

Table III. Cone Calorimetry Data of Neat PP and EA/APP/PP Composites

Sample	TTI (s)	PHRR1 (kW/m^2)	PHRR2 (kW/m^2)	Av-HRR (kW/m^2)	av-COY (kg/kg)	av-CO_2Y (kg/kg)	TSR (m^2/m^2)	Av-EHC (MJ/kg)
PP	41	996	/	293	0.05	2.92	1011	40
EA/APP/PP (1.25/23.75/75.00)	20	427	690	385	0.08	3.01	2553	47
EA/APP/PP (2.50/22.50/75.00)	17	352	431	284	0.07	2.90	2873	44
EA/APP/PP (3.75/21.25/75.00)	19	286	313	215	0.09	2.96	2784	44
EA/APP/PP (5.00/20.00/75.00)	18	220	217	174	0.08	2.92	2812	42
EA/APP/PP (6.25/18.75/75.00)	19	168	222	125	0.13	2.94	2480	39
EA/APP/PP (7.50/17.50/75.00)	16	150	167	106	0.12	2.95	'2199	37
EA/APP/PP (8.75/16.25/75.00)	12	272	132	119	0.14	2.90	1762	38

Table IV. Normalized Elemental Concentrations of the Char Surface

Sample	C (wt %)	O (wt %)	P (wt %)	N (wt %)
EA/APP/PP (1.25/23.75/75.00)	12.2	58.5	26.7	2.6
EA/APP/PP (2.50/22.50/75.00)	14.1	56.6	25.5	3.8
EA/APP/PP (3.75/21.25/75.00)	17.8	53.3	24.8	4.1
EA/APP/PP (5.00/20.00/75.00)	17.3	53.8	24.9	4.0
EA/APP/PP (6.25/18.75/75.00)	17.8	54.0	24.9	3.4
EA/APP/PP (7.50/17.50/75.00)	34.1	43.3	18.4	4.1
EA/APP/PP (8.75/16.25/75.00)	14.5	55.3	26.2	4.0

also contributed to the interaction between matrix and flame retardant, and promoted the formation of char layer at a lower temperature or at the initial burning stage. Therefore, the shortened TTIs did not result in the worse flame-retardant effect and instead corresponded to the demand of better flame-retardant performance.

Regarding the average yields of CO_2 (av-CO_2Y) and CO (av-COY) within 360 s, it can be seen in Table III that av-CO_2Y of EA/APP/PP composites showed a slight wave, but that the av-COY showed a clear rise with increasing the EA/APP mass ratio compared with neat PP. These results indicated that the addition of the IFR EA/APP promoted the incomplete combustion

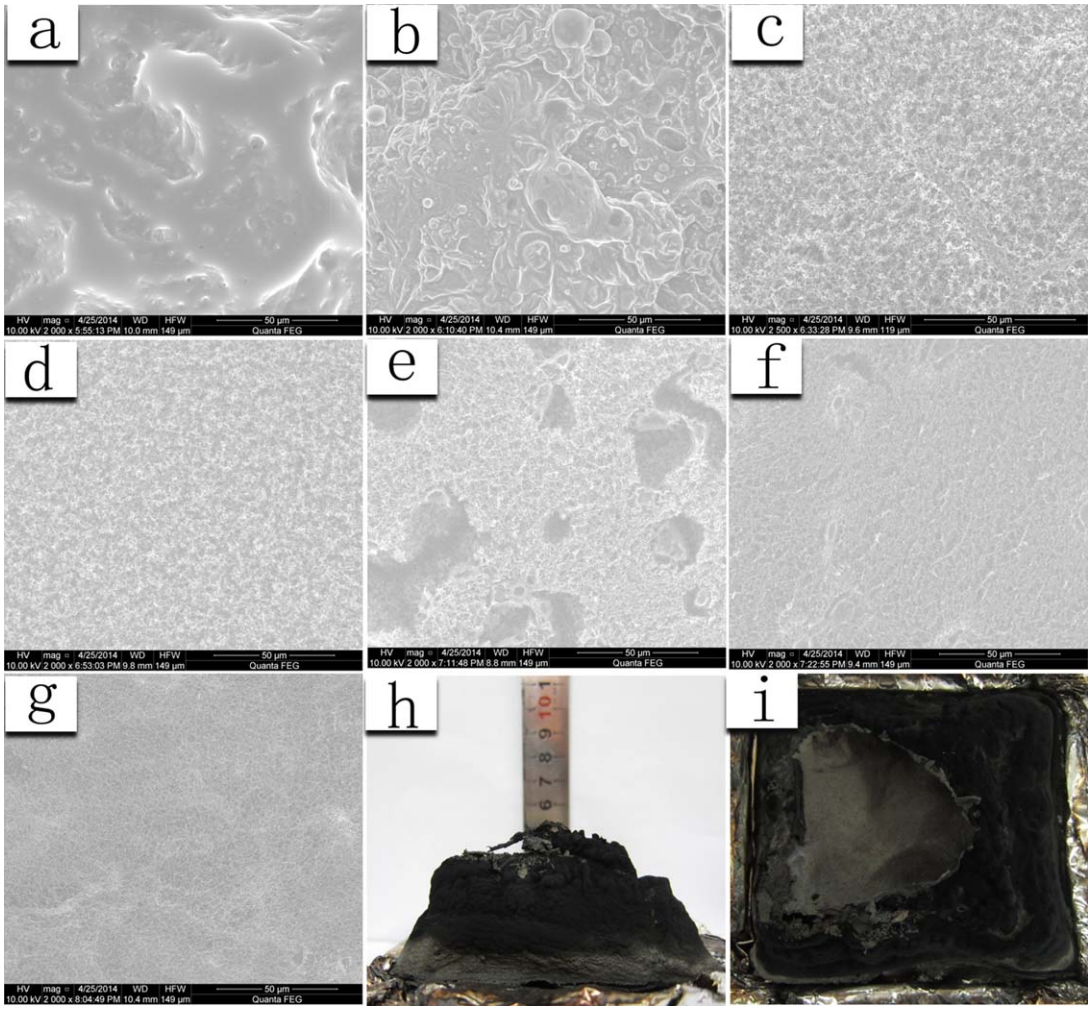

Figure 6. SEM images of EA/APP/PP composite (a–g) residues and digital photographs of charred residues obtained at the end of the cone calorimetry test (h, i). (a) EA/APP/PP(1.25/23.75/75.00), (b) EA/APP/PP(2.50/22.50/75.00), (c) EA/APP/PP(3.75/21.25/75.00), (d) EA/APP/PP(5.00/20.00/75.00), (e) EA/APP/PP(6.25/18.75/75.00), (f), (h), (i) EA/APP/PP(7.50/17.50/75.00), and (g) EA/APP/PP(8.75/16.25/75.00). [Color figure can be viewed in the online issue, which is available at wileyonlinelibrary.com.]

of composites, which further proved the gaseous-phase flame-retardant effect of EA/APP.

Total smoke release (TSR) is an indicative parameter of smoke. Table III shows that the TSR values of EA/APP/PP composites remarkably increased and reached the peak at 2873 m^2/m^2 (with 2.50/22.50 EA/APP mass ratio) but rapidly declined thereafter. However, all the TSR values of composites were still significantly higher than those of neat PP, which implied that the EA/APP/PP composites released more smog than neat PP. This phenomenon could be attributed to the explanation that the incorporation of EA/APP flame retardant led to insufficient combustion and thus formed unburned volatile char fragments, which was more obvious with the lack of charring agent (i.e., EA). Whereas the mass ratio of EA/APP flame retardant reached the appropriate value (i.e. 7.50/17.50), most of the char fragments were captured and became part of the intumescent char layer, and accordingly the TSR decreased obviously.

Morphology Analysis of Residues from Cone Calorimetry Test

The effect of the residue macroscopic morphology on flame retardancy was investigated using a digital camera and SEM. Figure 6(a–g) shows the SEM images of the EA/APP/PP residues after the cone calorimetry test. The residue of EA/APP/PP (1.25/23.75/75.00) composite in Figure 6(a) hardly showed any foaming on the surface of the char layer due to a few amounts of incorporated EA. Although the char layer of the EA/APP/PP (2.50/22.50/75.00) and EA/APP/PP (3.75/21.25/75.00) composites in Figure 6(b,c) showed slightly foaming, the foams were not adequately dense and had numerous holes, which resulted in poor performance in flame retardancy. The char layer of EA/APP/PP (5.00/20.00/75.00) and EA/APP/PP (6.25/18.75/75.00) composites in Figure 6(d,e) revealed denser foams but with several small holes and cracks, which still exhibited imperfect flame retardancy. Figure 6(f,h,i) shows that the residue of EA/APP/PP (7.50/17.50/75.00) composite displayed a perfect char layer with a intumescent, dense, and compact morphology, which prevented oxygen and heat exchange, and thus showed the best flame-retardant performance. The residue of EA/APP/PP (7.50/17.50/75.00) composite in Figure 6(g) exhibited the similar microscopic morphology as that of EA/APP/PP (7.50/17.50/75.00), which led to the better flame-retardant properties.

Chemical Structure of Residues from Cone Calorimetry Test

The normalized FTIR spectra of residues obtained from surface of char layer after cone calorimetry test were studied to better understand the synergic effect between EA and APP. Although the absorption peaks of all the residues in Figure 7 had similar appearances, several significant distinctions can be observed. The wide absorption peak at 3131 cm^{-1} was assigned to the —OH stretching vibration of P—OH and N—H in NH_4^+. The peak intensity was gradually enhanced with increasing EA/APP mass ratio, implying the formation of additional NH_4^+ groups between EA and APP. The interaction between EA and APP was thus vital in forming an intumescent flame-retardant effect. The peaks at 1155 and 992 cm^{-1} were assigned to the vibration of the P—O—C group, which indicated that crosslinking reactions among APP, EA, and PP occurred.[20] Furthermore, the peak

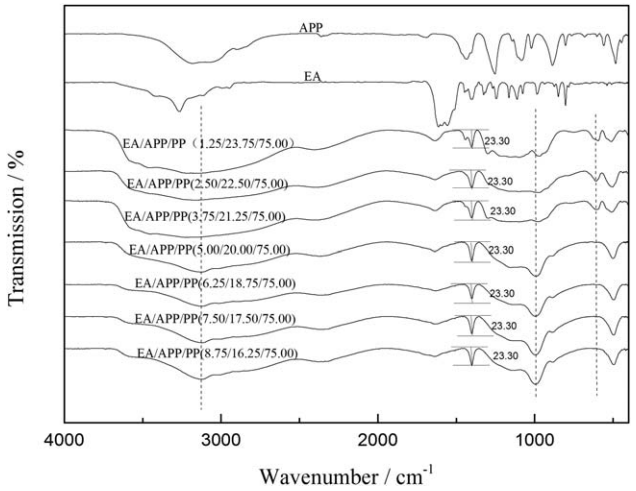

Figure 7. Normalized FTIR spectra of all residues from the cone calorimetry test.

intensities at 1155 and 992 cm^{-1} were also enhanced with increasing mass ratio EA/APP, indicating that more P—O—C structures were generated. These aforementioned changes implied the closely associated and complex chemical interaction among EA, APP, and PP. In addition, the absorption peak at 606 cm^{-1} corresponded to the out-of-plane bending vibration of —OH. When the mass ratio of EA/APP exceeded 15/85, the —OH peak vanished because the increased EA consumed more —OH groups. All the above results demonstrated that the synergistic effect between EA and APP occurred and was also strengthened with increasing EA/APP mass ratio.

Elemental Analysis of Residues from the Cone Calorimetry Test

Table IV shows the elemental contents of the EA/APP/PP residues from cone calorimetry test analyzed by XPS. The concentration of carbon element initially increased up to the maximum value of the EA/APP/PP (7.50/17.50/75.00) composite and then decreased with increasing EA/APP mass ratio. Additionally, the concentration of oxygen and phosphorus elements all initially decreased to the minimum of EA/APP/PP (7.50/17.50/75.00) composite and then increased instead. These results indicated that EA/APP with the appropriate mass ratio retained more carbon-containing constituents to form a char layer that can reduce flammable gas production and also effectively obstruct the diffusion of oxygen and heat. More importantly, the quality of elemental nitrogen in EA/APP/PP (7.50/17.50/75.00) residue reached the maximum value by calculating the product of the maximum residue quality and the residual maximum elemental mass ratio in residue. Results revealed that more nitrogen-rich chemical structures were captured in the residue. The more nitrogen-rich constituents combining with phosphorus-rich together promoted more carbon-rich constituents charring, which further implied the importance of the appropriate EA/APP mass ratio. Moreover, although the residues were obtained from the surface where combustion was most vigorous, the elemental concentrations still revealed that the appropriate EA/APP mass ratio can lock more carbon and nitrogen elements in the residue. The residue preserved more

constituents and thus promoted the enhancement of flame-retardant performance.

CONCLUSIONS

A hyperbranched triazine derivative charring agent (EA) was prepared. The IFR EA and AP with different mass ratio was incorporated into PP and prepared series of EA/APP/PP composites. Results of LOI, UL94, and cone calorimetry tests demonstrated that the intumescent flame-retardant EA/APP system effectively imposed flame retardancy to PP. Moreover, the EA/APP mass ratio clearly affected the flame-retardant properties of EA/APP/PP composites, and an optimal EA/APP mass ratio of 7.50/17.50 exerted the best flame-retardant effects on the composites, including the highest LOI value, UL94 V-0 ratings, lowest PHRR1 value, and highest residue char yield. An appropriate EA/APP mass ratio contributed to the interaction between EA and APP, and more nitrogen- and carbon-containing constituents interacted with phosphorus-containing constituents and were locked in the residue. Consequently, a compact and dense char layer formed. EA/APP at an appropriate mass ratio also possessed a gaseous-phase flame-retardant effect during the combustion of EA/APP/PP composite. In summary, the appropriate EA/APP mass ratio contributed to fully exerting both the optimal gaseous- and condensed-phase effects, which led to excellent flame-retardant performance of the EA/APP/PP composites.

ACKNOWLEDGMENTS

Beijing Technology and Business University Scientific Research Foundation for Young Teachers (No. QNJJ2011-48) and Education Science & Research Development Project of Beijing Municipal Institutions (No. KM201110011010).

REFERENCES

1. Gao, S. L.; Li, B.; Bai, P.; Zhang, S. Q. *Polym. Adv. Technol.* **2011**, *22*, 2609.
2. Demir, H.; Arkış, E.; Balköse, D.; Ülkü, S. *Polym. Degrad. Stab.* **2005**, *89*, 478.
3. Enescu, D.; Frache, A.; Lavaselli, M.; Monticelli, O.; Marino, F. *Polym. Degrad. Stab.* **2013**, *98*, 297.
4. Doğan, M.; Yılmaz, A.; Bayramlı, E. *Polym. Degrad. Stab.* **2010**, *95*, 2584.
5. Yang, K.; Xu, M. J.; Li, B. *Polym. Degrad. Stab.* **2013**, *98*, 1397.
6. Camino, G.; Costa, L.; Trossarelli, L. *Polym. Degrad. Stab.* **1984**, *7*, 243.
7. Camino, G.; Costa, L.; Trossarelli, L. *Polym. Degrad. Stab.* **1985**, *12*, 203.
8. Camino, G.; Martinasso, G.; Costa, L. *Polym. Degrad. Stab.* **1990**, *27*, 285.
9. Hu, X. P.; Li, W. Y.; Wang, Y. Z. *J. Appl. Polym. Sci.* **2004**, *94*, 1556.
10. Chen, Y. H.; Liu, Y.; Wang, Q.; Yin, H.; Aelmans, N.; Kierkels, R. *Polym. Degrad. Stab.* **2003**, *81*, 215.
11. Wang, G. J.; Huang, Y.; Hu, X. *Prog. Org. Coat.* **2013**, *76*, 188.
12. Li, X.; Ou, Y. X.; Zhang, Y. H.; Lian, D. *J. Chin. Chem. Lett.* **2000**, *11*, 887.
13. Huang, J. Q.; Zhang, Y. Q.; Yang, Q.; Liao, X.; Li, G. X. *J. Appl. Polym. Sci.* **2012**, *123*, 1636.
14. Pawelec, W.; Aubert, M.; Pfaendner, R.; Hoppe, H.; Wilén, C. E. *Polym. Degrad. Stab.* **2012**, *97*, 948.
15. Ren, S. J.; Fang, Q.; Lei, Y.; Fu, H. T.; Chen, X. Y.; Du, J. P.; Cao, A. *Macromol. Rapid Commun.* **2005**, *26*, 998.
16. Thach-Mien, D. N.; Chang, S. C.; Condon, B.; Uchimiya, M.; Graves, E.; Smith, J.; Easson, M.; Wakelyn, P. *Polym. Adv. Technol.* **2012**, *23*, 1036.
17. Blotny, G. *Tetrahedron* **2006**, *62*, 9507.
18. Qian, L. J.; Qiu, Y.; Liu, J.; Xin, F.; Chen, Y. J. *J. Appl. Polym. Sci.* **2014**, DOI: 10.1002/app.39709.
19. Qian, L. J.; Ye, L. J.; Qiu, Y.; Qu, S. R. *Polymer* **2011**, *52*, 5486.
20. Yin, H. Q.; Yuan, D. D.; Cai, X. F. *Polym. Degrad. Stab.* **2013**, *98*, 288.